On another level: the role of ubiquitination in endothelial inflammation

Drug Innovation

Research Profile

Jager, S. (Shelley)

Introduction

Inflammation is a part of the innate response to infection or tissue trauma. Acute inflammation is a fast and non-specific mechanism. Endothelial cells form the gateway between blood and areas of inflammation in the tissue and therefore play a pivotal part in vascular inflammation(1). Inflammatory stimuli affect endothelial functions such as dilation of the blood vessel, which increases local blood flow and decreased blood velocity; increased vascular permeability and leukocyte recruitment by upregulated cell-adhesion molecules such as E-selectin, VCAM-1, and ICAM-1; and clotting at the site of infection, initiated by the endothelial release of von Willebrand factor(VWF), to prevent the spread of pathogens via the blood (2–6).

There are two stages of endothelial cell activation: type I and type II. Type I activation is a rapid response mediated by G-protein coupled receptors, it does not require *de novo* protein synthesis or gene regulation. Type II activation results in a more sustained inflammatory state, it is mediated by pro-inflammatory cytokines, such as tumor-necrosis factor (TNF), and results in gene transcription and protein translation (1,7). Previously, our group has investigated the molecular response of endothelial cells to a range of cytokines through integration of multiple omics levels (phosphoproteome, transcriptome, and proteome)(8,9). We showed that TNFα and IFNγ induced unique inflammatory states in ECs. Moreover, TNFα and IFNγ signaling was synergistically enhanced through combined stimulation, potentially underlying effects which have been described other by studies (10–15).

The induction of these inflammatory states is dependent on the activation of specific transcription factors. TNFα mainly activates the NF-κB transcription factor through an intricate signaling cascade which is at the basis of regulating the expression of many inflammatory proteins and processes. For example, NFKB is responsible for the transcription of E-selectin, VCAM-1 and ICAM-1 in ECs. IFNγ activates the STAT transcription factors, through the JAK/STAT signaling pathway (16,17). The signaling cascades leading to activation of these transcription factors and gene transcription is highly complex and primarily driven by specific regulation of PTMs such as phosphorylation and ubiquitination(18–20).

Ubiquitination

Ubiquitination is the covalent linkage of one (mono-) or multiple (polyubiquitination) ubiquitin proteins to the epsilon-amine of lysine residues of the target protein. The ubiquitination system consist of ubiquitin-activating enzymes (E1), ubiquitin-conjugating enzymes (E2), ubiquitin ligases (E3), and ubiquitin-proteases (or deubiquitinases, DUBs)(21). Ubiquitin is a 76 amino acid protein containing 7 lysine residues (Lys6, 11, 27, 29, 33, 48, and 63), which, including the N-terminal methionine (M1), can all be ubiquitinated to form polyubiquitin chains(22). Ubiquitination is primarily associated with proteasomal degradation, however, different linkage types of polyubiquitination have been associated with different functions, including cell cycle control, protein trafficking and protein complex formation(23).

The role of ubiquitination in TNFα induced activation of the NFKB transcription factor is well-established. The response to TNFα is mediated by two TNF receptors: TNFR1 and TNFR2 (Figure 1). TNFR1 is expressed over all human tissue, while TNFR2 is primarily expressed in immune cells, neurons and endothelial cells(24,25). TNFR1 and TNFR2 have different intracellular domains, but their downstream signaling pathways possess both distinct and overlapping features.

NF-κB and JAK/STAT pathways

TNFR1 contains an intracellular death domain (DD), which interacts with a silencer of death domains (SODD). Upon TNFα binding, the SODD is released, and TNF-R1-associated death domain protein

(TRADD) and receptor interacting protein 1 (RIP1) are recruited (Figure 1A) (26). Polyubiquitination of RIP1 functions as molecular switch, as it enables recognition by the ubiquitin binding domain in the IκB kinase (IKK) and TAK1 kinase complexes (18,26). The IKK complex consists of IKKα, IKKβ and NEMO (NF-κB essential modulator), linear ubiquitin chain assembly complex (LUBAC) polyubiquitinates NEMO, which enhances phosphorylation and activation of IKKβ(27). This in turn enables phosphorylation and ubiquitination, leading to proteasomal degradation of NF-κB inhibitor IκBα, , which allows for NF-κB subunits, p50 and p65, to be translocated to the nucleus(28).

TNFR2 does not have a DD and interacts directly with TRAF1 and TRAF2. Similar to TNFR1 signaling, LUBAC is polyubiquitinated, which allows TAK1 and IKK recruitment, and ultimately translocation of NF-κB to the nucleus(18) (Figure 1B). TNFR2 can also trigger the non-canonical NF-κB pathway by activating NF-κB inducing kinase (NIK). NIK is primarily ubiquitinated by TRAF/cIAP complexes and is thereby targeted for proteasomal degradation. However, upon TNFα stimulation these complexes are recruited by the TNFα receptor and NIK is not degraded but activated. This results in in the nuclear translocation of the p52/relB complex(29,30).

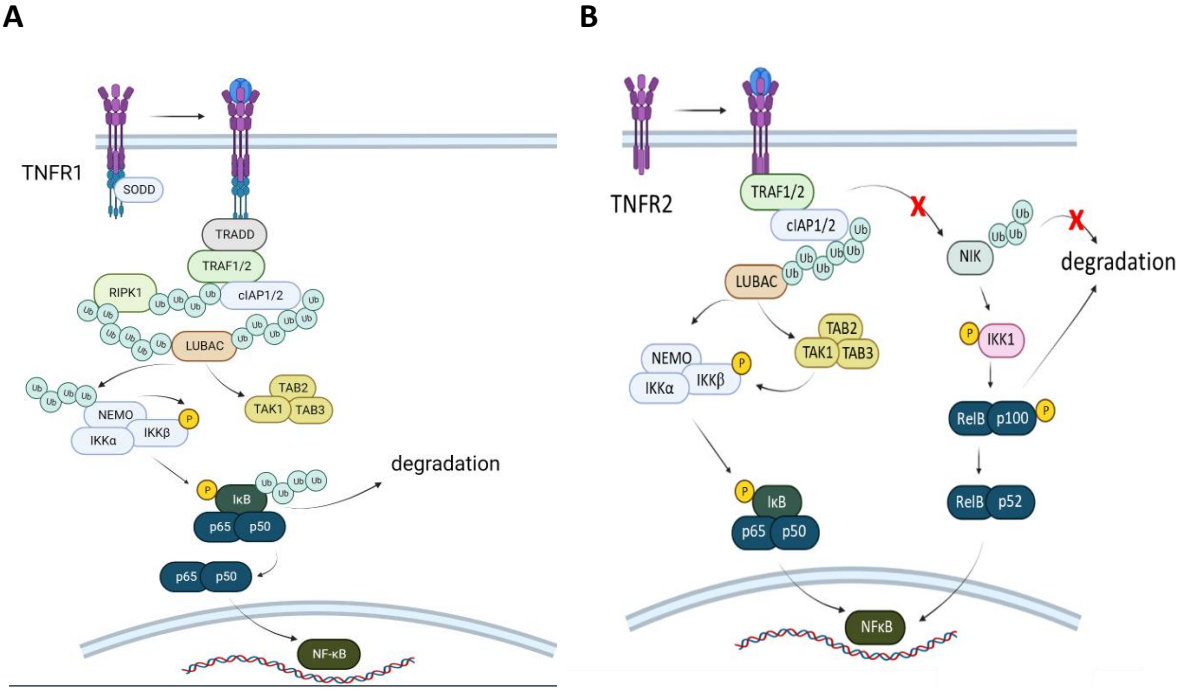

Figure 1: The signaling pathway upon activation of (A) TNFR1 and (B) TNFR2. *A) TNFR1 recruits TRADD and RIP1. RIP1 is ubiquitinated by cIAPs and TRAF1, 2, or 5. Ubiquitinated RIP1 is then recognized by the ubiquitin binding domain of the TAK1 and IKK complex. Ubiquitination of NEMO by LUBAC allows for phosphorylation of IKKβ, and ubiquitination and subsequent degradation of IκBα, to allow translocation to the nucleus for p50 and p65(RelA). B) TNFR2 directly interacts with TRAF1/2, and activates* NF-κB *in a similar fashion as TNFR1. TNFR2 also activates the non-canonical* NF-κB *pathway. As NIK is no longer ubiquitinated and degraded, it can phosphorylate IKK1, which ultimately leads to translocation of the RelB/p52 complex to the nucleus. Figure adapted from Lousa et al. (2022)*(18)*.*

The role of ubiquitination in the JAK/STAT pathway is not as well established compared to its role in the NF-κB pathway. However, negative regulation of the JAK/STAT pathway occurs through proteasomal degradation, initiated by ubiquitination(31,32). Moreover, the crosstalk between the JAK/STAT and NF-κB pathways might be regulated through ubiquitylation. For example, it has been found that TRAF6, an E3 ligase that plays an important role in NF-κB activation by activating IKKs, also interacts with STAT3(33). Additionally, activation of the JAK-STAT1/2 pathway lead to increased levels

of the E3 ligase TRIM22(34), which inhibits autoubiquitination of TRAF6, thereby inhibiting the TRAF6-stimulated activation of NF-κB (35).

Ubiquitin profiling

Analysis of ubiquitylation requires enrichment before MS analysis, which can be achieved by protein-centric and peptide-centric enrichment. Protein-centric enrichment is performed on the intact proteome after cell lysis, this can be achieved through the expression of affinity tagged ubiquitin, or by using ubiquitin-specific antibodies or ubiquitin-binding traps. However, the gold standard method for ubiquitylation profiling is by targeting the diGly (or K-GG, or K-ε-GG) remnant peptides(21). The C-terminus of ubiquitin, which sequence starts with GGR (Gly-Gly-Arg) is covalently attached to the e-amine group of lysine residues, thus after tryptic digestion, which cleaves at the C-terminal side of arginine, two glycines, a diGly, remain (Figure 2). This results in a mass increment of 114.043 Da, which is detectable by MS(21).

A

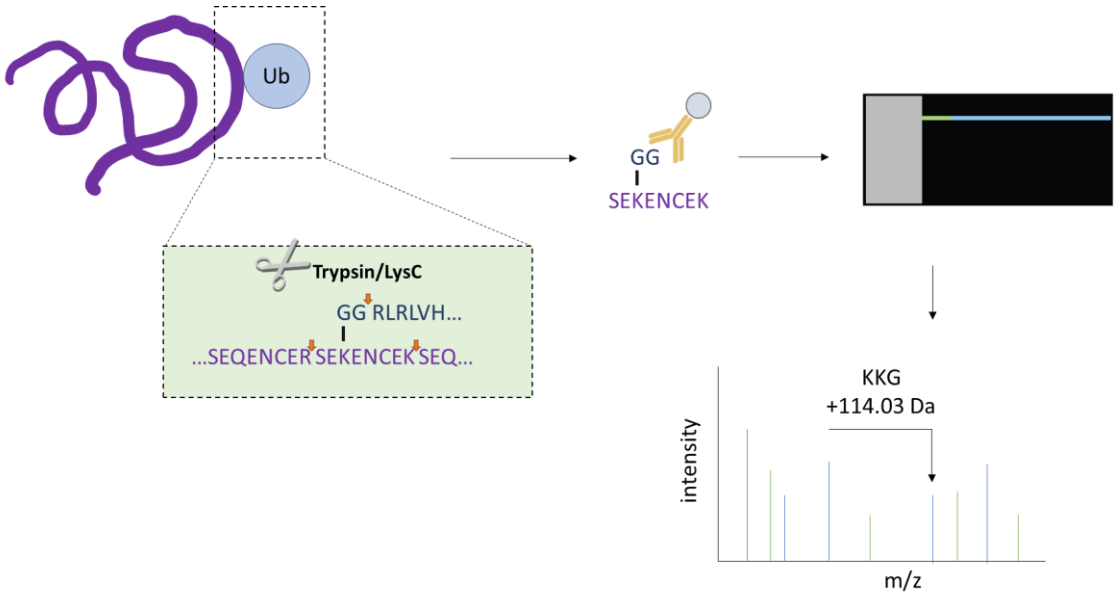

B

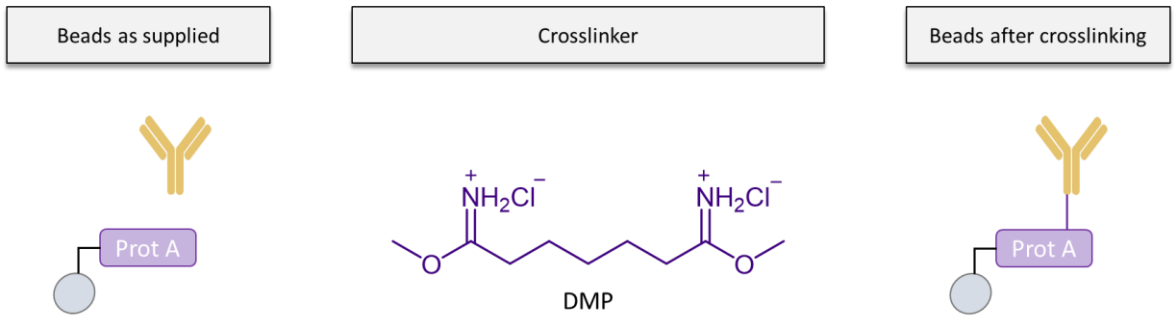

Figure 2: Peptide-centric enrichment for ubiquitin profiling. *A) Upon digestion with trypsin/LysC, the ubiquitin is cleaved off the protein backbone, leaving 2 glycines. This diGly motive can be recognized with specific antibodies and thereby enriched. These enriched peptides can be analyzed with mass spectrometry and the diGly motive will lead to a mass shift of 114.03 Da. B) The beads we have used are supplied as a mixture of antibody and protein A beads. We have used the crosslinker DMP to covalently link the antibody and the protein A.*

A major disadvantage of diGly peptide enrichment is the requirement for large sample amounts (15 mg per sample). Acquiring these large amounts are labor and cost extensive, especially considering experiments with multiple conditions and replicates. In 2013, Udeshi *et al.* published a protocol for diGly enrichment with only 5-10 mg of protein(36). This protocol starts with crosslinking the protein A coupled Sepharose beads and antibody to obtain a covalent bond, which reduces contamination of the eluted fraction with antibody (Figure 2B). More recently, this group published another study using the same crosslinked beads, but requiring only 1 mg of peptides starting material(37). In this study, quantification of the ubiquitin sites was achieved by TMT labelling, which could be performed directly on bead. Additionally, two other recent studies have used the crosslinked beads for ubiquitin remnant motive enrichment, which were analyzed by data-independent acquisition and quantified in a label-free manner(38,39). Both start with 1-2 mg peptide material.

Here, we will use the same protocol as described by the studies mentioned before, which involves the crosslinking of the antibody to the protein A-beads, to develop a robust and accurate proteomic workflow for ubiquitin profiling in endothelial cells. This method will then be applied to study the role of ubiquitination in the endothelial inflammatory response to TNFα.

Methods

Cell culture

Blood outgrowth endothelial cells (BOECs) were isolated and cultured as described(40). BOECs derived from four individual donors were pooled and used for the analysis of the ubiquitination profiling of the endothelial response to TNFα.

Cell stimulation and lysis

Cells were grown to confluency on collagen coated 150 mm plates. TNFα was added to a total concentration of 10 ng/ml, the plate was carefully swirled to ensure that the TNFα is sufficiently mixed throughout the plate. Control plates were only swirled, without any addition. For each sample, two plates were stimulated and combined. After 15 min incubation at 37 ℃, cells were washed three time with PBS and subsequently lysed by scraping in SDC lysis buffer (1% SDC, 40 mM CAA, 10 mM TCEP, 100 mM Tris, pH 8, supplemented with HALT phosphatase and protease inhibitor cocktail (Thermo Scientific)). Lysates were boiled for 5 min and sonicated for 10 min, then stored at -80 ℃.

Crosslinking anti-K-e-GG antibody

The PTM-Scan ubiquitin remnant motif (K-e-GG) kit (Cell Signaling Technologies) was crosslinked as described with minor modifications(36). In short, non-covalently bound antibody and beads were washed three times with 100 mM sodium borate (pH 9.0) before a 1 h incubation with 20 mM DMP at room temperature. The crosslinking reaction was quenched by washing twice with 100 mM TRIS/HCl (pH 8), followed by a 2 h incubation with 100 mM TRIS/HCl at room temperature. Beads were either washed 3x with PBS and stored at 4 ℃ in PBS; or used directly. Crosslinking was always performed in batches of 40 μL beads (1 vial from the PTM-Scan kit).

Sample preparation and K-e-GG enrichment

Proteins were digested by incubating them overnight with Trypsin/LysC (1:100-200 enzyme-to-protein ratio) (Thermo Scientific) at 37 ℃. TFA was added to the sample to a final concentration of 1%. Then, peptides were desalted on SDB-RPS cartridges (AffiniSep) in 4 mg batches. First, cartridges were equilibrated with 1 mL methanol, followed by 1 mL 1% TFA in water. Samples were loaded and subsequently washed three times with 1 mL 0.2% FA. Peptides were eluted with 750 μL 80% ACN/5% ammonium hydroxide. Peptides were dried by vacuum centrifugation and stored at -20 ℃.

Dried peptides were resuspended in immunoaffinity buffer (IAP) (50 mM MOPS, pH 7.2, 10 mM Na_2HPO_4, 50 mM NaCl). Peptide concentrations were estimated using the Pierce™ Quantitative Peptide Assays (Thermo Scientific). Crosslinked beads were transferred to spin columns and washed with 800 μL IAP buffer (50 xg, 30 s, followed by 200 xg, 1.5 min). Peptides were added to the beads and incubated 6 h to overnight at 4 ℃. Flowthrough was collected by centrifugation (50 g, 30 s, followed by 100 g, 5 min). Then, column was washed twice with ice-cold IAPS, followed by two washed of ice-cold MS H_2O (50 xg, 30 s, followed by 200 xg, 1.5 min). DiGly peptides were eluted with 10 column volumes of 0.2% FA (50 g, 30 s, followed by 200 g, 1.5 min), in three consecutive steps.

Peptide clean-up for MS analysis

Peptides of diGly enrichment flowthrough and collection fractions were either desalted using in-house prepared C18 stage tips or loaded directly onto Evotips (EvoSep) if the EvoSep LC platform was used. C18 stage tips were conditioned in three consecutive steps: 50 μL MeOH, 50 μL 80% ACN/3% TFA, and 50 μL MS H_2O (700 xg, 1 min, after each step), followed by loading of the sample (300 xg, 5 min). Tips were washed three times with 50 μL 0.5% acetic acid (700 xg, 1 min) and subsequently eluted in three consecutive steps with 20 μL 80% ACN/0.5% acetic acid (300 xg, 5 min). Evotips were equilibrated, loaded and washed as described by the manufacturer(41). In short, tips were soaked in isopropanol, and then washed with ACN/0.1% FA, equilibrated with 0.1% FA. Samples were loaded and washed with 0.1% FA. The tips were submerged in 0.1% FA to prevent drying.

LC-MS/MS analysis

For all optimization experiments, separation of peptides was achieved by nanoscale C18 reverse chromatography on an Ultimate 3000 HPLC system (Thermo Fisher Scientific) coupled on-line to an Orbitrap Fusion Tribrid mass spectrometer (Thermo Fisher Scientific). Mobile-phase solvent A consisted of 0.1% FA in MS water, and mobile-phase solvent B consisted of 0.1% FA in ACN. The flow rate was 300 nL/min. A 60 min gradient was used. The sample was loaded for 17 minutes, after which peptides were eluted by gradually increasing the concentration of solvent B. For ubiquitin peptides, solvent B was first increased from 2.5% to 7% (17-26 min), from 7% to 20% (26-75 min), from 20% to 36% (75-114 min), from 36% to 45% (114-124 min), followed by a 5-minute wash (95%, 124-138 min), and equilibration to 2.5% at 153 min. For proteome samples and flowthrough, solvent B was kept at 5% (17-22 min), then increased from 5% to 17% (22-100 min), from 17% to 38% (100-147 min), from 38% to 90% (147-157 min), followed by a 5-minute wash (90%, 157-162 min), and equilibration to 5% over 5 minutes (162-167 min). Data was collected in a data-dependent fashion. The scan-range was set to 300-1600 *m/z*, the resolution was 60000 (@ *m/z* 200) and the maximum injection time was 50 ms. Filters for tandem mass spectrometry were set to include change states 2-7, dynamic exclusion was set to 30 s, and the 15 highest precursors were selected for fragmentation. Isolation was performed with the quadrupole, with the isolation window set to 0.7 *m/z*, higher energy collisional dissociation (HCD) fragmentation at 28% and a resolution of 30000 (@ *m/z* 200). All data were acquired with Xcalibur software (Thermo Fisher Scientific).

The peptides for the ubiquitin profiling of TNFα stimulated endothelial cells were separated using the Evosep One (Evosep) LC system with the standard 88-minute gradient, which was coupled on-line to an Orbitrap Fusion Lumos Tribrid mass spectrometer (Thermo Fisher Scientific). The mass spectrometry method was the same as describe above with the following adaptions: the MS1 resolution was 120000 (@ m/z 200), the filters for MS2 selection include only charge state 2-4, dynamic exclusion was set to 20 s, data dependent mode was set to 1 sec, and HCD energy was 33%.

Raw data analysis

Raw data was analyzed with MaxQuant (2.0.1) using the default settings with match between runs (MBR) enabled. Carbamidomethyl (C) was defined as fixed modification and the variable modifications were Oxidation (M), Acetyl (Protein N-term), and GlyGly (K). Data was matched to the human proteome database from UniProt (2019).

Bioinformatic processing

Data analysis was performed in RStudio. DiGly sites were filtered for a localization probability > 0.5, and data was filtered to contain >50 % valid values in at least one condition. Intensities were log2 transformed and missing values were imputed based on a Gaussian normal distribution with a width of 0.3 and a downshift of 1.8. Statistical testing was performed using LIMMA(42). Gene ontology enrichment was performed using http://www.geneontology.org/ and protein networks were made using https://www.string-db.org/. Network maps were made in Cytoscape (version 3.9.1). E3 ligase activity profiling was performed with UbE3-APA(43).

Results

Ubiquitin enrichment optimization

An initial pilot experiment was performed to determine whether the previous described protocols are optimal for ubiquitin profiling in our existing model for endothelial inflammation. Thus, BOECs were either stimulated with TNFα for 1 h, or left untreated, and then lysed and digested using a combination of trypsin and LysC and subsequently desalted, while the remaining was loaded onto the crosslinked beads In total we collect three different fractions: the proteome before enrichment, the enrichment flowthrough, and the enriched fraction (Figure 3A). Before loading samples onto the beads, we checked crosslinking of the antibody to the beads on SDS-page gel (Supplemental Figure S1). Due to peptide loss in sample workup 500 μg peptides were loaded onto the beads. We were able to identify approximately 40000 peptides in the proteome and flowthrough samples, and 10000 in the enriched sample (Figure 4B). Of these, approximately 100 K-e-GG peptides were found in the non-enriched samples, while 800 were found in the enriched samples (Figure 4B).

Although there was a slight enrichment of diGly peptides compared to non-enriched fractions, the enrichment efficiency was below 10%, which is drastically lower compared to literature (60-70% (44,45)). It was described by Steger *et al.* that the amount of K-e-GG peptides identified decreased drastically if less than 1 mg of peptide material was loaded onto the affinity resin(44), which could explain low diGly peptide yields

A

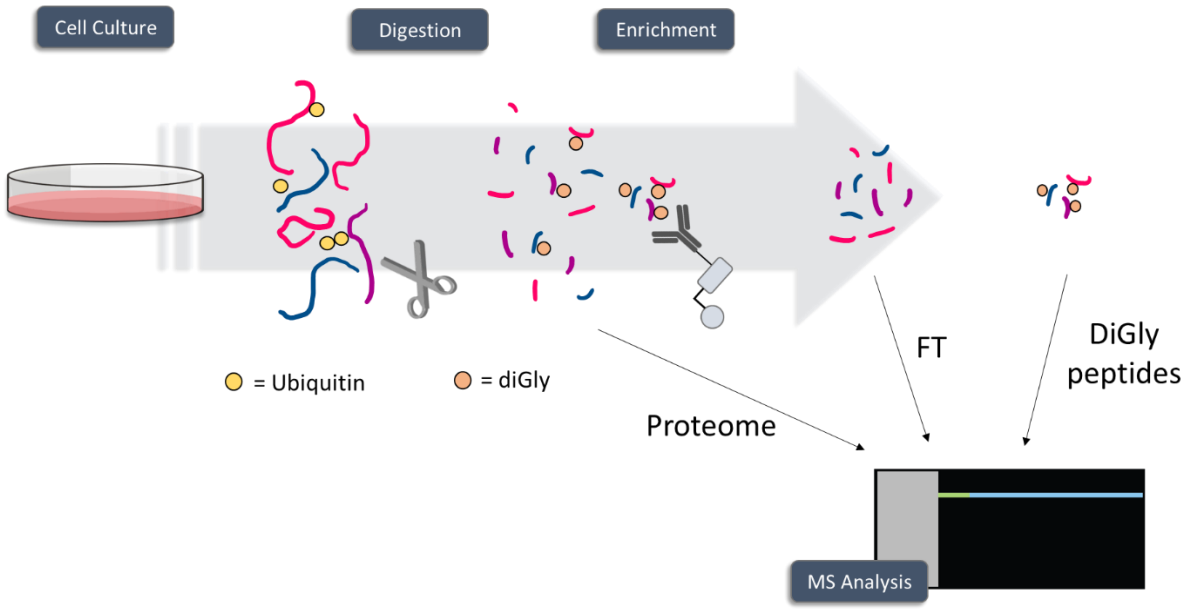

B

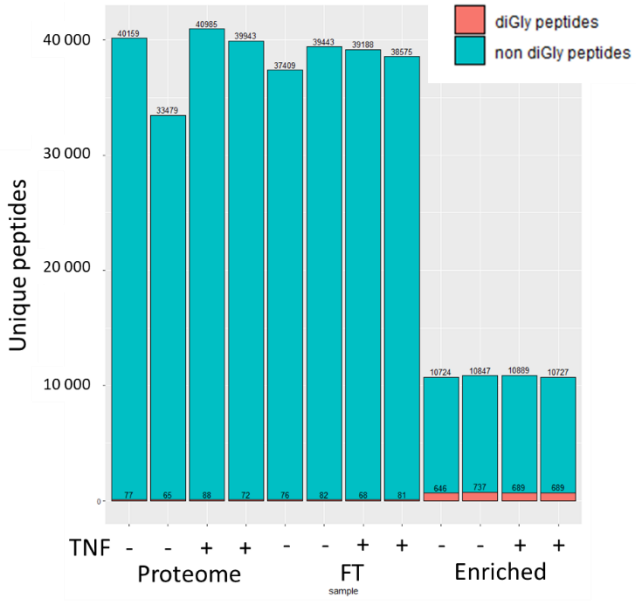

Figure 3: A) Workflow for the enrichment of ubiquitylated peptides. *The cell lysate is digested with Trypsin/LysC, and subsequently desalted. From here, a sample is taken to analyze the whole proteome. The desalted peptide mixture is enriched for diGly peptides using the specific antibody matrix. Enriched and flow-through (FT) peptides are desalted and analyzed with MS. B) Results of the first pilot experiment. Plotted are the number of unique peptides in each sample that contain a diGly modification (orange) and that do not contain a diGly modification (blue).*

As diGly-peptide enrichment is highly dependent on starting material, we first aimed to optimize required peptide amounts to yield increased enrichment. In total, 12 150 mm plates of were pooled and digested with Trypsin/LysC, resulting in a starting amount of 42 mg peptides. After desalting, 20

mg of peptide remained. Of this, 10 mg was loaded onto 60 µL 50% affinity beads and 4 mg was loaded onto 20 µL 50% affinity beads (Figure 4A). In the enriched fractions, approximately 13000 peptides were identified, of which 2115 and 1753 diGly peptides, in the 10 and 4 mg samples, respectively (Figure 4). Although this was a 2-fold increase compared to the previous experiment, it remains multi-fold lower compared to the approximately 20,000 peptides others achieve using the same enrichment strategy. Moreover, enrichment efficiency was still only 15 % regardless of starting amount. (39,44).

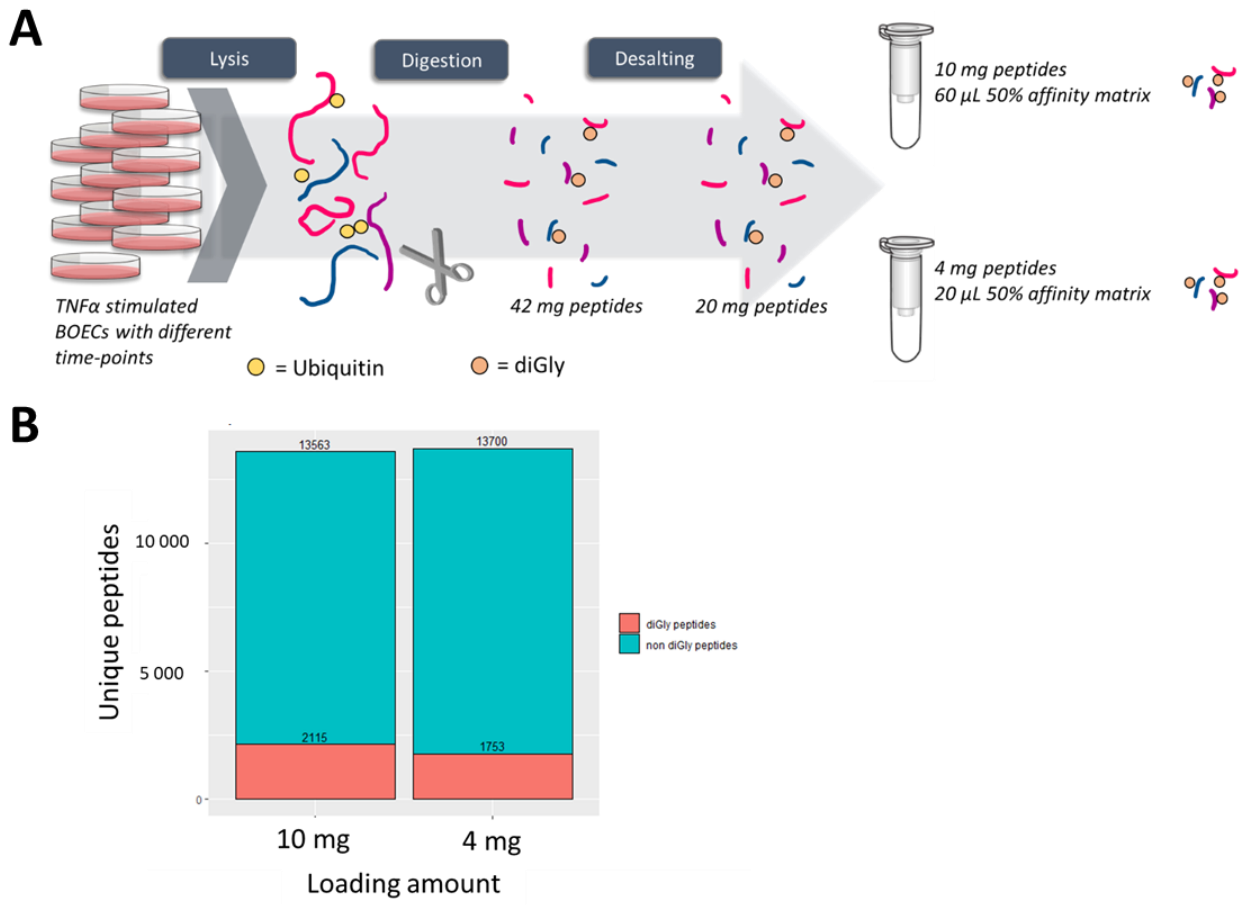

Figure 4: enrichment optimization. *A) workflow describing the optimization efforts. Different lysates from different cells batches stimulated with* TNFα *were taken and pooled. This was digested with Trypsin/LysC, resulting in 42 mg peptides. After desalting, 20 mg peptides remained. B) The number of unique peptides with (orange) and without (blue) diGly modification.*

As our enrichment efficiency remained low, we also investigated the LC-MS method to understand whether we could increase the absolute number of identifications. For the previous experiments we used an LC gradient of 100 minutes for the enriched samples as a starting point while a 125-minute gradient was used for the proteome and flow through samples. It is generally assumed that a longer gradient will increase the number of identified peptides(46), especially in data-dependent acquisition. Using the 100-minute gradient, most diGly peptides were identified within the first 60 minutes of the gradient (Figure 5), thus we initially tested a decreased gradient slope to increase diGly peptide separation.

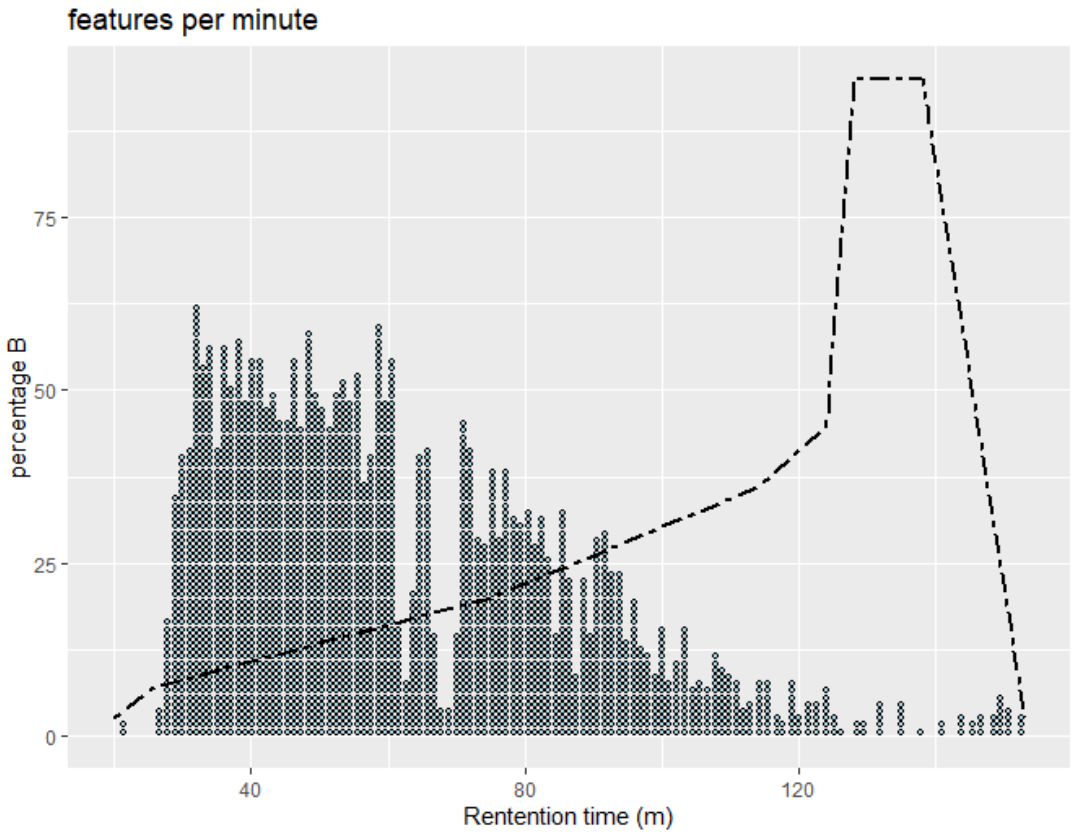

Figure 5: DiGly peptides identified over time. *Each dot represents a unique sequence of a diGly peptide, the bin width was set to 1 minute. The dashed line represents the gradient in percentage of solvent B. Note that the gradient starts from t = 17 minutes, as the first 17 minutes are the loading of the sample.*

The 10 mg enriched sample from the loading amount optimization was taken and diluted 3 times to allow 3 new injections for MS analysis. Three new LC methods were tested: method 1, the original 100-minute gradient; method 2, the 125-minute gradient used in our proteome and flowthrough analysis; and method 3, a method with decreased slope between 5 and 17 % solvent B (Figure 6A). As the concentration was 3-fold lower than in the previous experiment, there were overall less identified peptides and less diGly peptides. However, with a longer method the absolute number of unique identified diGly peptides was doubled compared to the 100-minute gradient (Figure 6B).

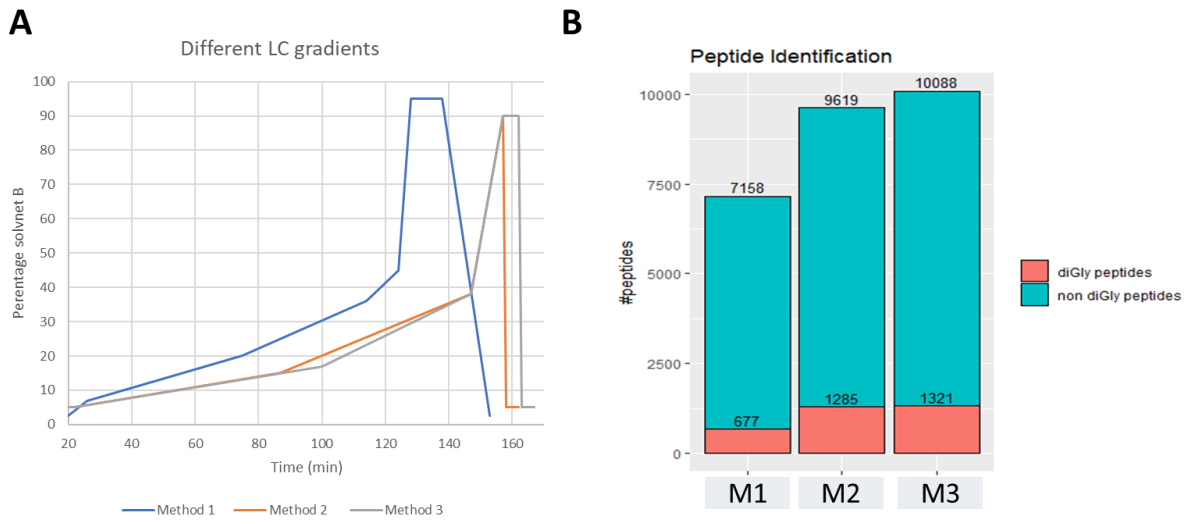

Figure 6: LC gradient optimization. *A) A graph displaying the change in percentage of solvent B over time in the different methods. Note that the peptides elute mostly between 5 and 45% solvent B, when the percentage of solvent B is above that threshold it is considered as a wash to clean the column. B) The number of unique peptides with (orange) and without (blue) diGly modification. M1 = Method 1, M2 = Method 2, M3 = Method 3.*

Ubiquitination profiling in endothelial inflammation after TNFα stimulation

To analyze the initial ubiquitin signaling signatures in TNFα induced endothelial stimulation, BOECs were treated with TNFα for 15 minutes, after which we performed the ubiquitin enrichment and proteomic analysis. This time window allows for result comparison with the study of Hansen *et al.* (45), who used a similar TNFα stimulation window, as well as a comparison to our previous phosphoproteome data(9).

As the previous optimizations demonstrated no added benefit in starting with 10 mg peptides, compared to 4 mg, we aimed to use a similar 4 mg of starting material. We used three biological replicates per condition and each sample was injected twice to reduce missing values. Unfortunately, enrichment was not successful in one replicate of each condition and therefore we omitted these samples (Supplemental Figure S2). Across the remaining samples, the total number of unique identified peptides was between 19000 and 24000, of which 1800 to 2000 unique diGly peptides (Figure 7A). The enrichment efficiency was approximately 10% in each sample, and approximately 90% of diGly peptides were identified in both injection replicates (Figure 7B). To gain a better understanding of the overall quality of this set, we created a correlation matrix of every run in this sample (Figure 7C). Firstly, we examined the intensity distribution of the different identified peptides. The density plots (Figure 7C, diagonal) show that the intensity of the identified diGly peptides is either similar or higher than the intensities of the non diGly peptides. Then, we examined the correlation between injection replicates and biological replicates. It would be expected that the highest correlation would be between the injection replicates, however, for good label free quantification, a high correlation of intensities throughout biological replicates is required as well. Indeed, the correlation coefficients between injection replicates and the overall correlation between biological replicates are always above 0.9. Additionally, the scatterplots show only a small spread between these replicates, especially at the higher peptide intensities. Overall, the correlation between diGly peptides of all samples is high, suggesting limited differences between the conditions.

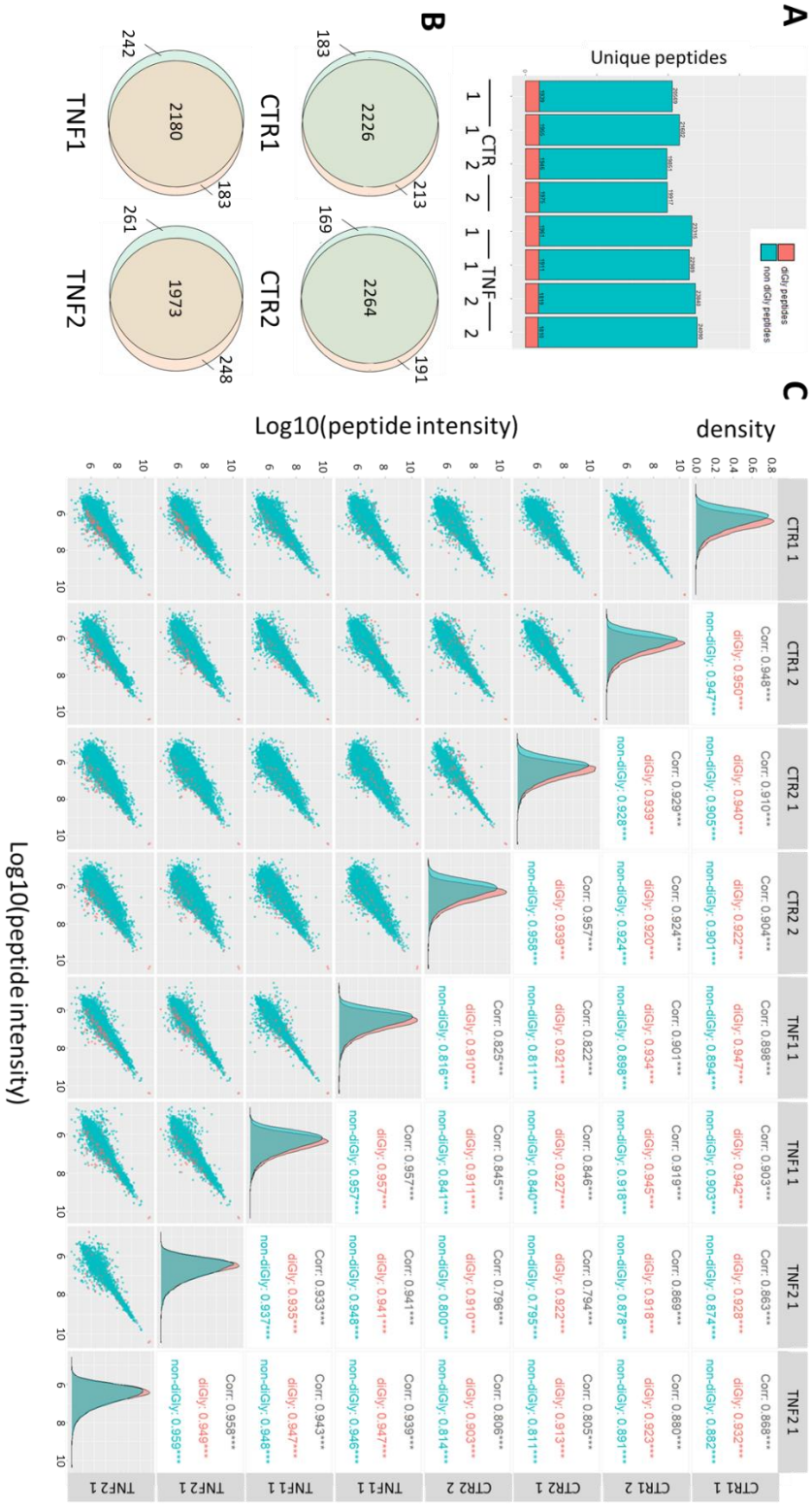

Figure 7: Peptide identifications in ubiquitin profiling in response to TNFα. *A) The number of unique identified peptides with (orange) and without (blue) diGly modification. B) Venn diagrams displaying diGly peptides found in each injection replicate in each biological replicate. C) Correlations between each dataset, with in the bottom: scatterplots of the log10 intensity of peptides in each sample (orange = diGly peptides, blue = non-diGly peptides), on the diagonal: density plots (orange = diGly peptides, blue = non-diGly peptides), and on top the correlation coefficient of all data points (black), all diGly peptides (orange), and all non-diGly peptides (blue).*

To understand the TNFα signaling events we assessed the obtained ubiquitination sites. First, we looked at ubiquitin itself, as it should be highly abundant and were able to identify all lysine linkage types on ubiquitin in each sample, which appear to have similar abundances with and without TNFα stimulation (Supplemental Figure S3). However, due to limitations in our raw data analysis software which does not allow for diGly annotation on the N-terminus, we were not able to identify N-terminal diGly modifications on ubiquitin that are responsible for linear polyubiquitination. Then, we sought to identify changes upon TNFα stimulation (Figure 8A). After performing a t-test on the raw peptide intensities, we identified 7 upregulated and 11 downregulated ubiquitin sites (FDR = 5%). The upregulated sites after TNFα stimulation include: RIPK1 K604, BIRC2 (cIAP1) K448, and IKBKG (NEMO) K277 (Figure 8B); which are all known to be ubiquitinated upon NF-κB activation by TNFα (18).Apart from these three sites, ubiquitination of SLC23A2, a vitamin C transporter, is increased. It was previously found that the activity of SLC23A2 is decreased in intestinal epithelial cells upon TNFα stimulation(47), and our findings suggest that ubiquitination may play a role in this. The other upregulated sites found were: CCDC18 (coiled coil domain containing 18), RPS6KC1 (ribosomal protein S6 kinase C1), and RHBDF1 (rhomboid 5 homolog 1). These proteins have not previously been linked to TNFα signaling.

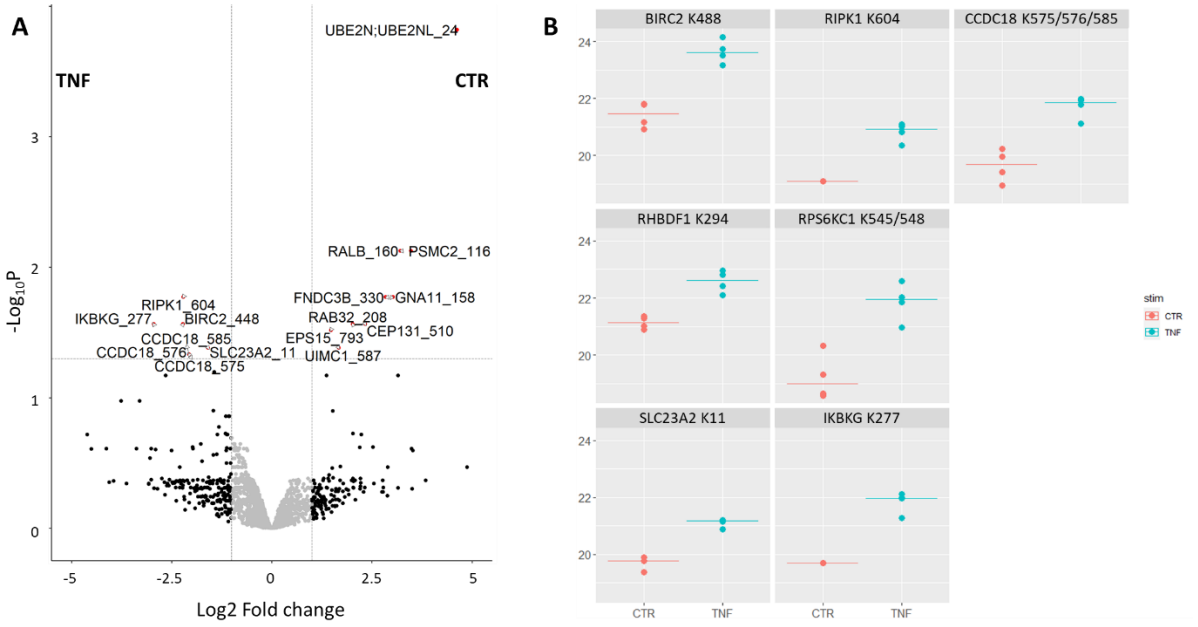

Figure 8: quantitative analysis of ubiquitination upon TNFα induced endothelial inflammation*. A) Volcano plot of the ubiquitinome after TNFα stimulation. Up- and downregulated sites (LIMMA, 5% FDR, log2 fold change > 1) are colored in red. B) Log2 intensities of the upregulated sites with the lowest P-value, the horizontal bar represent the median value. C) Log2 intensities of the downregulated sites with the lowest P-value, the horizontal bar represents the median value.*

To investigate both the ubiquitination and phosphorylation signaling events in related to NF-κB signaling through TNFR1 and TNFR2 signaling we performed a gene ontology enrichment (GO:0051092, GO:0007249, GO:1901222, and GO:0032088). We used the phosphorylation site data after 10 min TNFα stimulation from previously acquired data(9). Enrichment revealed 97 ubiquitin and 113 phosphorylation sites related to this signaling cascade, which were mapped both in an interaction network (Figure 9). This analysis shows specific ubiquitin and phosphorylation signatures, for example when looking at the proteins within the LUBAC, IKK, and TAK/TAB complex (Supplemental Figure S4). As previously mentioned, we identify upregulated ubiquitin on RIPK1 and BIRC2 (cIAP2), following the signaling pathway described in Figure 1A, this leads to upregulated ubiquitin and phosphorylation on LUBAC, which will activate this complex, resulting in ubiquitination on the TAK/TAB complex and NEMO (IKBKG), which is in agreement with our data.

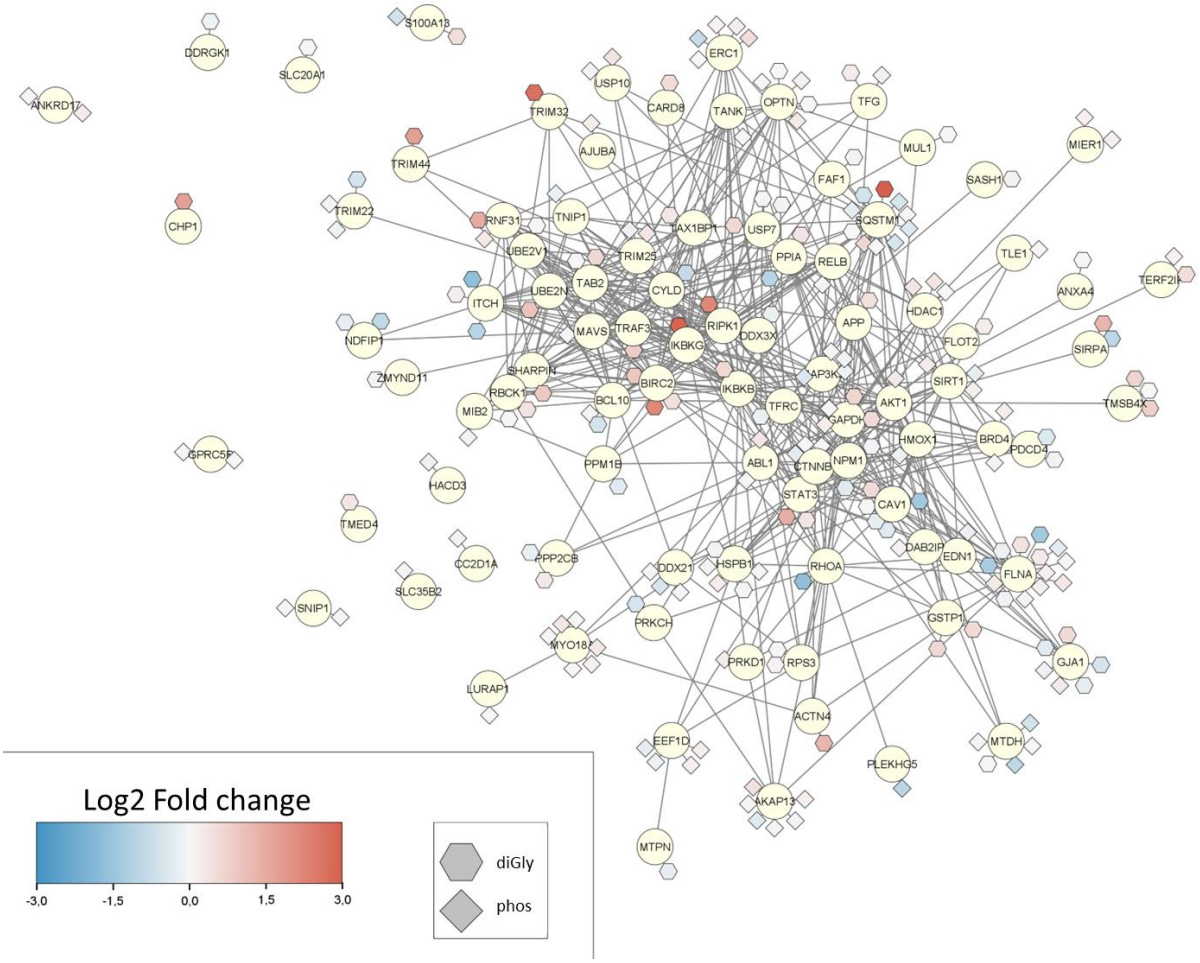

Figure 9: Ubiquitination and phosphorylation in TNFα induced endothelial inflammation. *Protein network of all identified ubiquitin and phosphorylation sites in proteins within the NF-κB signaling. Hexagons represent the different ubiquitin sites, diamonds represent phosphorylation sites, and their color represents the log2 fold change in intensity.*

To assess which ligases are responsible for the observed ubiquitination sites we employed UbE3-APA software that allows for the profiling of E3 ubiquitin ligase activity from diGly analysis data(43). This revealed 21 E3 ligases with upregulated activity and 1 E3 ligase with downregulated activity (Figure 10A). Activation of these ligases might be the consequence of phosphorylation or ubiquitination, thus, we analyzed both this ubiquitinome and the previously analyzed phosphoproteome to find matches for these E3 ligases (Figure 10B-C). Four of these E3 ligases were ubiquitinated at 15 minutes, of which

BIRC2 K448 ubiquitination was found to be upregulated compared to control, and four E3 ligases were found to have phosphorylation sites, however this was not different from control.

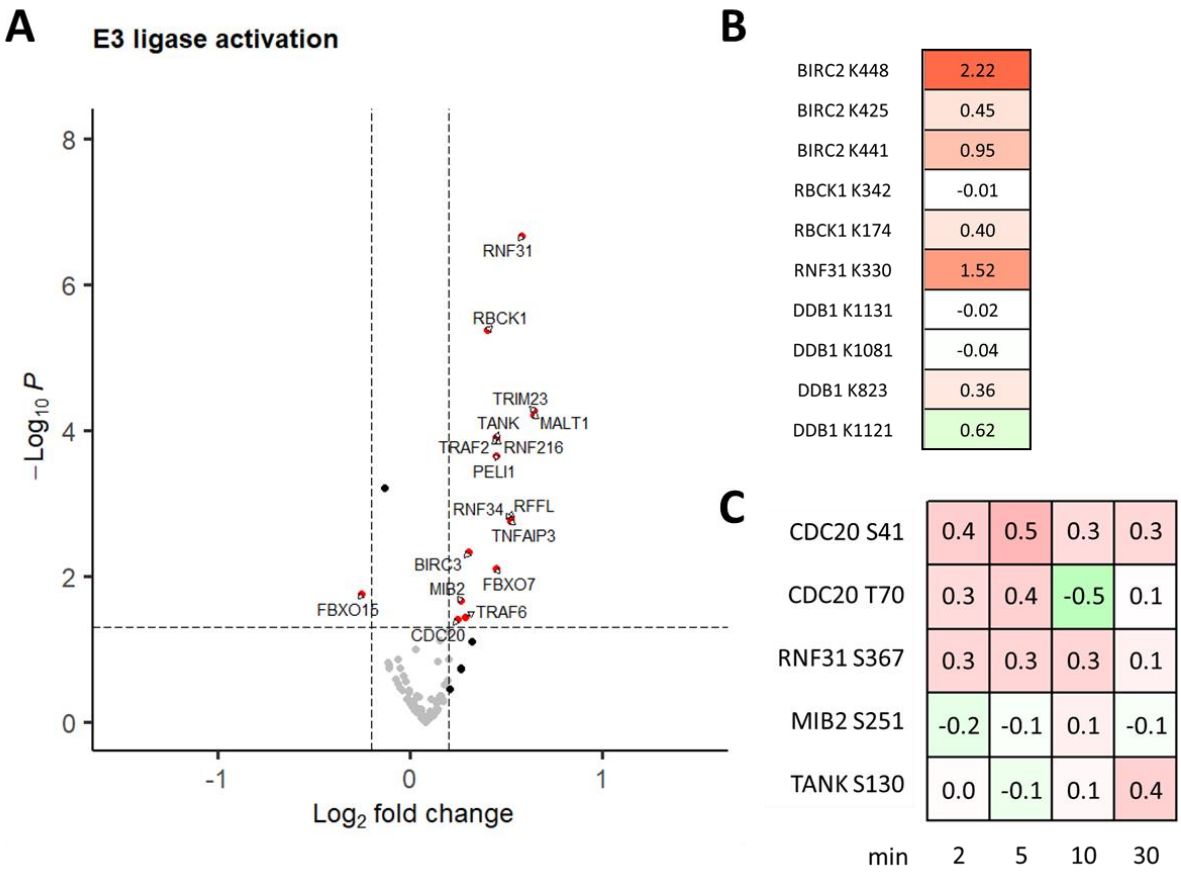

Figure 10: E3 ligase activation after TNFα stimulation. *A) Volcano plot of E3 ligase activation. The Log2 fold change cut-off was set to 0.2 and the -log P value cut-off was set to 0.05. The E3 activation output from UbE3-APA revealed 21 ligases with upregulated activity and 1 with downregulated activity. B) Different abundance of ubiquitin sites of the in A shown E3 ligases after 15 minutes of TNFα stimulation. C) Different abundance of phosphorylation sites of the in A shown E3 ligases between 2 and 30 minutes.*

Discussion

Overall, we have optimized and used a method to study ubiquitination in endothelial cells. We show that the starting peptide amount for diGly enrichment can be decreased by crosslinking the protein A beads to the diGly specific antibody, in consensus with previous reports(36,37,44,45). Using MS analysis, we were able to identify approximately 2000 diGly sites per sample, which is 4-to-10-fold lower than reported by others. However, we were able to identify almost 100 ubiquitin sites on proteins within the NF-κB signaling, of which well-known ubiquitinated targets: RIPK1, cIAP2, and TAB2, and members of the LUBAC complex. We also used UbE3-APA, a software tool to profile the activity of E3 ligases. This revealed 21 E3 ligases with upregulated activity.

Our method still yielded a low enrichment efficiency (approximately 10%), compared to reported efficiencies (60-70% (44,45)). However, these reported efficiencies were all obtained using proteasome inhibitor MG-132, thus increasing the total amount of ubiquitination in a cell. When applying their method on a biological system without inhibitor, the enrichment efficiency drops to 25%(45). This is

still higher than the 10% we reached; thus, further optimization would be beneficial to increase the enrichment efficiency. For example, decreasing the affinity matrix may lead to saturation of the antibodies, which may in turn decrease non-specific binding. Proteasome inhibitors may be used for method optimization or as a positive control. However, for the analysis of biological systems, proteasome inhibition will not portray the actual biological situation.

Furthermore, the quantification strategy should be improved to gain more confidence. Here, we used the raw peptide intensity to quantify their abundances. However, the peptide intensity is relative to the total loading amount into the mass spectrometer, and does not provide a robust quantification method, especially with this small sample size. The incorporation of labels might improve the accuracy of the quantification. For example, stable isotope labelling by amino acids in cell culture (SILAC), or tandem mass tag (TMT) labelling can be applied. TMT-labelling can be performed on bead and in the flow-through separately, as has been described by others(37,48). A few drawbacks of labelling are that it increases the amount of sample steps and reagent required are often expensive. Robust label free quantification can be achieved if features are found across all replicates, which is where data-independent acquisition (DIA) might offer opportunities, which is less susceptible to run-to-run variability(49). However, DIA requires different data analysis software, as MaxQuant is less equipped to analyze this data, and DIA-NN (specific analysis software for DIA data) has not been widely-used for diGly profiling(44).

Even with these limitations we have shown that it is possible to identify key ubiquitous interactions within upon TNFα stimulation in endothelial cells. It would be interesting to extend this with IFNγ and TNFα-IFNγ-co-stimulation. It has for example been described that the ubiquitous interactions of TRAF6, TRIM22 and STAT3 result in an interplay of the NF-kB and JAK/STAT pathways(33–35). In our E3 ligase activity profiling, TRAF6 was found to have upregulated activity, and we identified 2 ubiquitin sites on STAT3 with higher intensity in TNFα stimulated cells. Therefore, it would be interesting to see whether this is also the case upon IFNγ and co-stimulation.

One last point of interest is the co-existence of different PTMs on a single protein, which cannot be analyses with peptide-centric analysis. It would be interesting to pull-down specific protein or the entire NF-kB complex and analyze the PTMs involved on an intact or native level. As our data shows, some proteins can be phosphorylated and ubiquitinated at multiple sites and examining these proteins will show whether these regulatory PTMs exist together. We have tried to set-up this experiment with immunoprecipitation of NF-kB, however, we were not able to obtain a repeatable protocol for this enrichment.

Conclusion

In summary, our data shows that ubiquitination is an important and high occurring PTM in the endothelial inflammatory response to TNFα. Although we identify less sites, our results are in line with other ubiquitination profiling efforts in response to TNFα in other cell types. Optimization of the method might be beneficial to increase the number of identifications and provide robust quantification.

References:

1. Hunt BJ, Jurd KM. Endothelial cell activation: A central pathophysiological process. BMJ Br Med J. 1998 May 5;316(7141):1328.
2. Hannoodee S, Nasuruddin DN. Acute Inflammatory Response. Nature. 2021 Nov 21;206(4979):20.
3. Ortega-Gómez A, Perretti M, Soehnlein O. Resolution of inflammation: an integrated view. EMBO Mol Med. 2013 May;5(5):661.
4. Kenneth Murphy CW. Janeway's Immunobiology. 9th editio. 2017. 904 p.
5. Pober JS, Sessa WC. Evolving functions of endothelial cells in inflammation. Nat Rev Immunol 2007 710. 2007 Oct;7(10):803–15.
6. Dmitrieva NI, Burg MB. Secretion of von Willebrand factor by endothelial cells links sodium to hypercoagulability and thrombosis. Proc Natl Acad Sci U S A. 2014 Apr 29;111(17):6485–90.
7. Xiao L, Liu Y, Wang N. New paradigms in inflammatory signaling in vascular endothelial cells. Am J Physiol - Hear Circ Physiol. 2014 Feb 1;306(3):317–25.
8. Béguin EP, van den Eshof BL, Hoogendijk AJ, Nota B, Mertens K, Meijer AB, et al. Integrated proteomic analysis of tumor necrosis factor α and interleukin 1β-induced endothelial inflammation. J Proteomics. 2019;192(June 2018):89–101.
9. Groten SA, Smit ER, Janssen EFJ, van den Eshof BL, van Alphen FPJ, van der Zwaan C, et al. The endothelial inflammatory repertoire: a multi-omics delineation of cytokine induced endothelial inflammatory states. *under review*: Cell Reports. 2022;
10. Ohmori Y, Schreiber RD, Hamilton TA. Synergy between Interferon-γ and Tumor Necrosis Factor-α in Transcriptional Activation Is Mediated by Cooperation between Signal Transducer and Activator of Transcription 1 and Nuclear Factor κB. J Biol Chem. 1997 Jun 6;272(23):14899–907.
11. Mehta NN, Teague HL, Swindell WR, Baumer Y, Ward NL, Xing X, et al. IFN-γ and TNF-α synergism may provide a link between psoriasis and inflammatory atherogenesis. Sci Rep. 2017;7(1):13831.
12. Karki R, Sharma BR, Tuladhar S, Williams EP, Zalduondo L, Samir P, et al. Synergism of TNF-α and IFN-γ Triggers Inflammatory Cell Death, Tissue Damage, and Mortality in SARS-CoV-2 Infection and Cytokine Shock Syndromes. Cell. 2021 Jan 1;184(1):149.
13. Mehta NN, Teague HL, Swindell WR, Baumer Y, Ward NL, Xing X, et al. IFN-γ and TNF-α synergism may provide a link between psoriasis and inflammatory atherogenesis. Sci Rep. 2017 Oct 23;7(1):13831.
14. Barcia C, Ros CM, Annese V, Gómez A, Ros-Bernal F, Aguado-Year C, et al. IFN-γ signaling, with the synergistic contribution of TNF-α, mediates cell specific microglial and astroglial activation in experimental models of Parkinson's disease. Cell Death Dis. 2011 Apr 7;2(4):e142–e142.
15. Foss S, Bottermann M, Jonsson A, Sandlie I, James LC, Andersen JT. TRIM21—From intracellular immunity to therapy. Front Immunol. 2019;10(AUG):2049.
16. Delgoffe GM, Vignali DAA. STAT heterodimers in immunity: A mixed message or a unique signal? JAK-STAT. 2013 Jan 1;2(1):e23060.
17. Majoros A, Platanitis E, Kernbauer-Hölzl E, Rosebrock F, Müller M, Decker T. Canonical and non-canonical aspects of JAK-STAT signaling: Lessons from interferons for cytokine responses.

Front Immunol. 2017 Jan 26;8(JAN):29.

18. Lousa I, Reis F, Santos-Silva A, Belo L. The Signaling Pathway of TNF Receptors: Linking Animal Models of Renal Disease to Human CKD. 2022;

19. Silke J. The regulation of TNF signalling: what a tangled web we weave. Curr Opin Immunol. 2011 Oct;23(5):620–6.

20. Harhaj EW, Dixit VM. Deubiquitinases in the regulation of NF-κB signaling. Cell Res 2011 211. 2010 Nov 30;21(1):22–39.

21. Steger M, Karayel Ö, Demichev V. Ubiquitinomics: history, methods and applications in basic research and drug discovery. Proteomics. 2013 Mar 30;1–25.

22. Swatek KN, Komander D. Ubiquitin modifications. Nat Publ Gr. 2016;26:399–422.

23. Yau R, Rape M. The increasing complexity of the ubiquitin code. Vol. 18, NATURE CELL BIOLOGY. 2016.

24. Medler J, Wajant H. Tumor necrosis factor receptor-2 (TNFR2): an overview of an emerging drug target. Expert Opin Ther Targets. 2019;23(4):295–307.

25. Holbrook J, Lara-Reyna S, Jarosz-Griffiths H, McDermott M. Tumour necrosis factor signalling in health and disease. F1000Research 2019 8111. 2019 Jan 28;8:111.

26. Humphries F, Yang S, Wang B, Moynagh PN. RIP kinases: key decision makers in cell death and innate immunity. Cell Death Differ. 2015;

27. Smit JJ, Van Dijk WJ, El Atmioui D, Merkx R, Ovaa H, Sixma TK. Target Specificity of the E3 Ligase LUBAC for Ubiquitin and NEMO Relies on Different Minimal Requirements. J Biol Chem. 2013 Nov 11;288(44):31728.

28. Yu H, Lin L, Zhang Z, Zhang H, Hu H. Targeting NF-κB pathway for the therapy of diseases: mechanism and clinical study.

29. Rauert H, Wicovsky A, Müller N, Siegmund D, Spindler V, Waschke J, et al. Membrane Tumor Necrosis Factor (TNF) Induces p100 Processing via TNF Receptor-2 (TNFR2). J Biol Chem. 2010 Mar 5;285(10):7394–404.

30. Sun SC. Non-canonical NF-κB signaling pathway. Cell Res 2011 211. 2010 Dec 21;21(1):71–85.

31. Linossi EM, Nicholson SE. Critical Review The SOCS Box-Adapting Proteins for Ubiquitination and Proteasomal Degradation.

32. Croker BA, Kiu H, Nicholson SE. SOCS Regulation of the JAK/STAT Signalling Pathway. Semin Cell Dev Biol. 2008;19(4):414.

33. Wei J, Yuan Y, Jin C, Chen H, Leng L, He F, et al. The ubiquitin ligase TRAF6 negatively regulates the JAK-STAT signaling pathway by binding to STAT3 and mediating its ubiquitination. PLoS One. 2012 Nov 19;7(11).

34. Wang Y, Chen Y, Lin Y, Quan Y, Xiao X, Zhang R. TRIM22 inhibits respiratory syncytial virus replication by targeting JAK-STAT1/2 signaling. J Med Virol. 2021 Jun 1;93(6):3412–9.

35. Qiu H, Huang F, Xiao H, Sun B, Yang R. TRIM22 inhibits the TRAF6-stimulated NF-κB pathway by targeting TAB2 for degradation. Virol Sin. 2013 Aug;28(4):209.

36. Udeshi ND, Mertins P, Svinkina T, Carr SA. Large-scale identification of ubiquitination sites by mass spectrometry. Nat Protoc. 2013 Oct;8(10):1950–60.

37. Udeshi ND, Mani DC, Satpathy S, Fereshetian S, Gasser JA, Svinkina T, et al. Rapid and deep-scale ubiquitylation profiling for biology and translational research. Nat Commun. 2020 Dec 1;11(1).

38. Steger M, Ihmor P, Backman M, Müller S, Daub H. Deep ubiquitination site profiling by single-shot data-independent acquisition mass spectrometry. bioRxiv. 2020 Jul 24;2020.07.23.218651.

39. Hansen FM, Tanzer MC, Brüning F, Bludau I, Stafford C, Schulman BA, et al. Data-independent acquisition method for ubiquitinome analysis reveals regulation of circadian biology. Nat Commun 2021 121. 2021 Jan 11;12(1):1–13.

40. Martin-Ramirez J, Hofman M, Van Den Biggelaar M, Hebbel RP, Voorberg J. Establishment of outgrowth endothelial cells from peripheral blood. Nat Protoc 2012 79. 2012 Aug 23;7(9):1709–15.

41. Bache N, Geyer PE, Bekker-Jensen DB, Hoerning O, Falkenby L, Treit P V, et al. A Novel LC System Embeds Analytes in Pre-formed Gradients for Rapid, Ultra-Robust Proteomics. 2018;

42. Ritchie ME, Phipson B, Wu D, Hu Y, Law CW, Shi W, et al. limma powers differential expression analyses for RNA-sequencing and microarray studies. Nucleic Acids Res. 2015;43(7).

43. Gong Y, Chen Y. UbE3-APA: a bioinformatic strategy to elucidate ubiquitin E3 ligase activities in quantitative proteomics study. Bioinformatics. 2022 Apr 12;38(8):2211–8.

44. Steger M, Demichev V, Backman M, Ohmayer U, Ihmor P, Müller S, et al. Time-resolved in vivo ubiquitinome profiling by DIA-MS reveals USP7 targets on a proteome-wide scale. Nat Commun. 2021;12(1).

45. Hansen FM, Tanzer MC, Brüning F, Bludau I, Stafford C, Schulman BA, et al. Data-independent acquisition method for ubiquitinome analysis reveals regulation of circadian biology. Nat Commun 2021 121. 2021 Jan 11;12(1):1–13.

46. Hsieh EJ, Bereman MS, Durand S, Valaskovic GA, MacCoss MJ. Effects of Column and Gradient Lengths on Peak Capacity and Peptide Identification in nanoflow LC-MS/MS of Complex Proteomic Samples. J Am Soc Mass Spectrom. 2013 Jan;24(1):148.

47. Subramanian VS, Sabui S, Subramenium GA, Marchant JS, Said HM. Tumor necrosis factor alpha reduces intestinal vitamin C uptake: a role for NF-B-mediated signaling Said HM. Tumor necrosis factor-reduces intestinal vitamin C uptake: a role for NF-B-mediated signaling. Am J Physiol Gastro-intest Liver Physiol. 2018;315:241–8.

48. Abelin JG, Bergstrom EJ, Taylor HB, Rivera KD, Olive ME, Clauser KR, et al. MONTE enables serial immunopeptidome, ubiquitylome, proteome, phosphoproteome, acetylome analyses of sample-limited tissues. bioRxiv. 2021;

49. Gillet LC, Navarro P, Tate S, Röst H, Selevsek N, Reiter L, et al. Targeted Data Extraction of the MS/MS Spectra Generated by Data-independent Acquisition: A New Concept for Consistent and Accurate Proteome Analysis*. undefined. 2012;11(6).

Supplemental Figures

S1

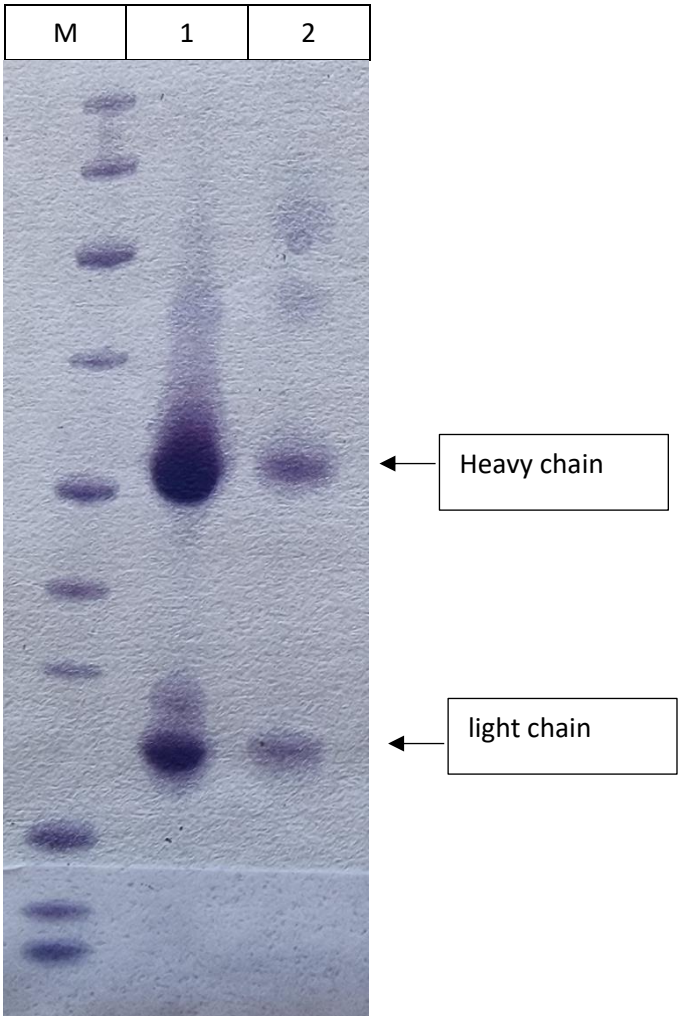

Figure S1: crosslinking of protein A bead to diGly antibody. Sample before (1) and after (2) crosslinking was taken, boiled in DTT and SDS sample buffer, then run on an SDS page gel. The intensity of the antibody after crosslinking is lower, as the antibody is now bound to the bead and no longer elutes in the gel.

S2

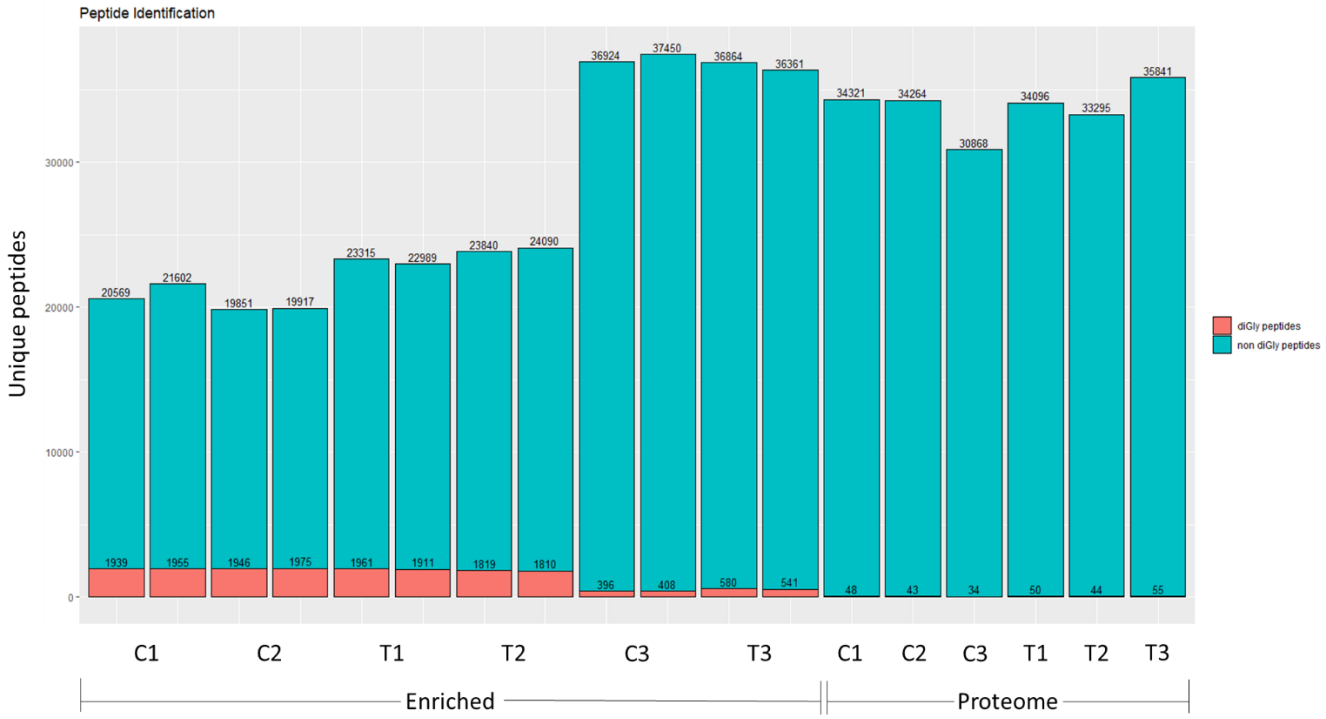

Supplementary Figure S2: Peptide identifications in ubiquitin profiling upon TNFα stimulation. As the enrichment of C3 and T3 was not successful, these samples were omitted from the analysis.

S3

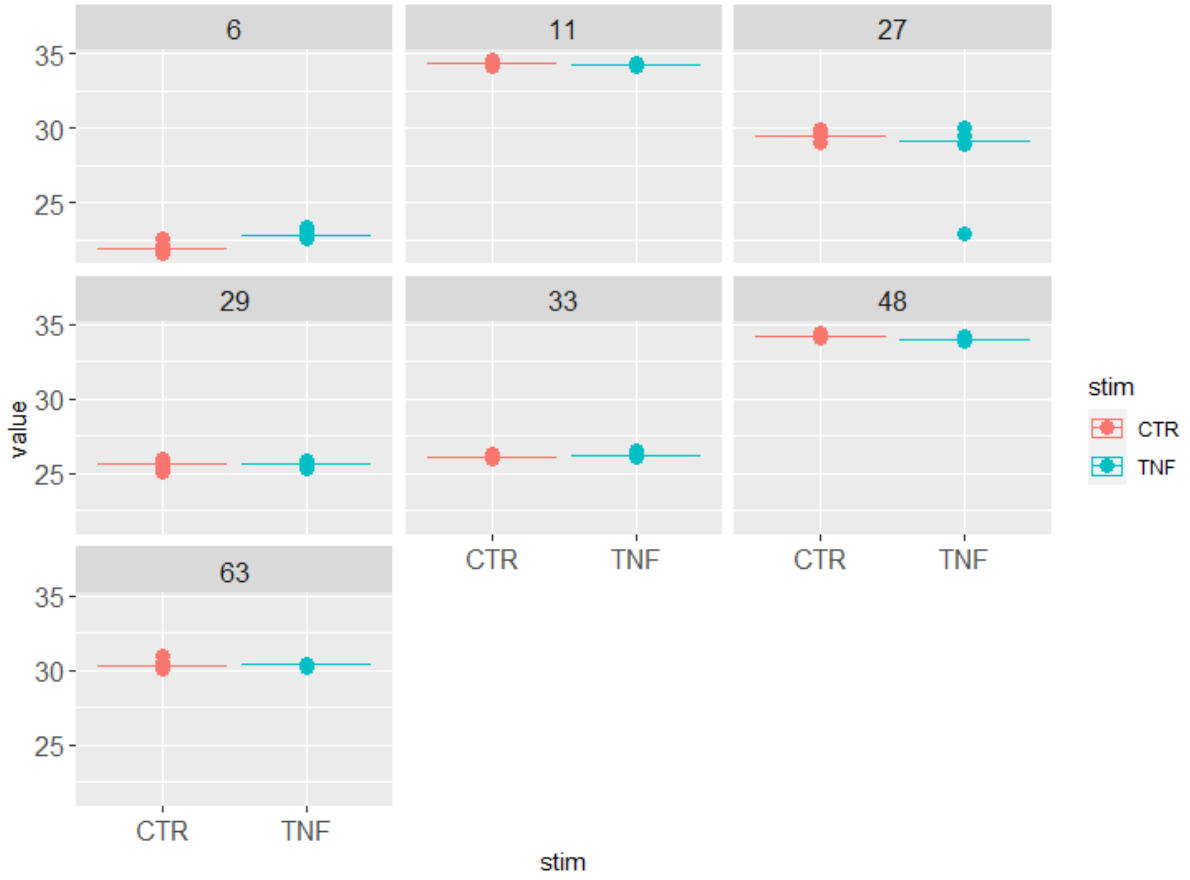

Supplementary Figure S3: different Ubiquitin linkages found. All 7 lysine linkages are found, abundances do not seem different between stimulated and control samples.

S4

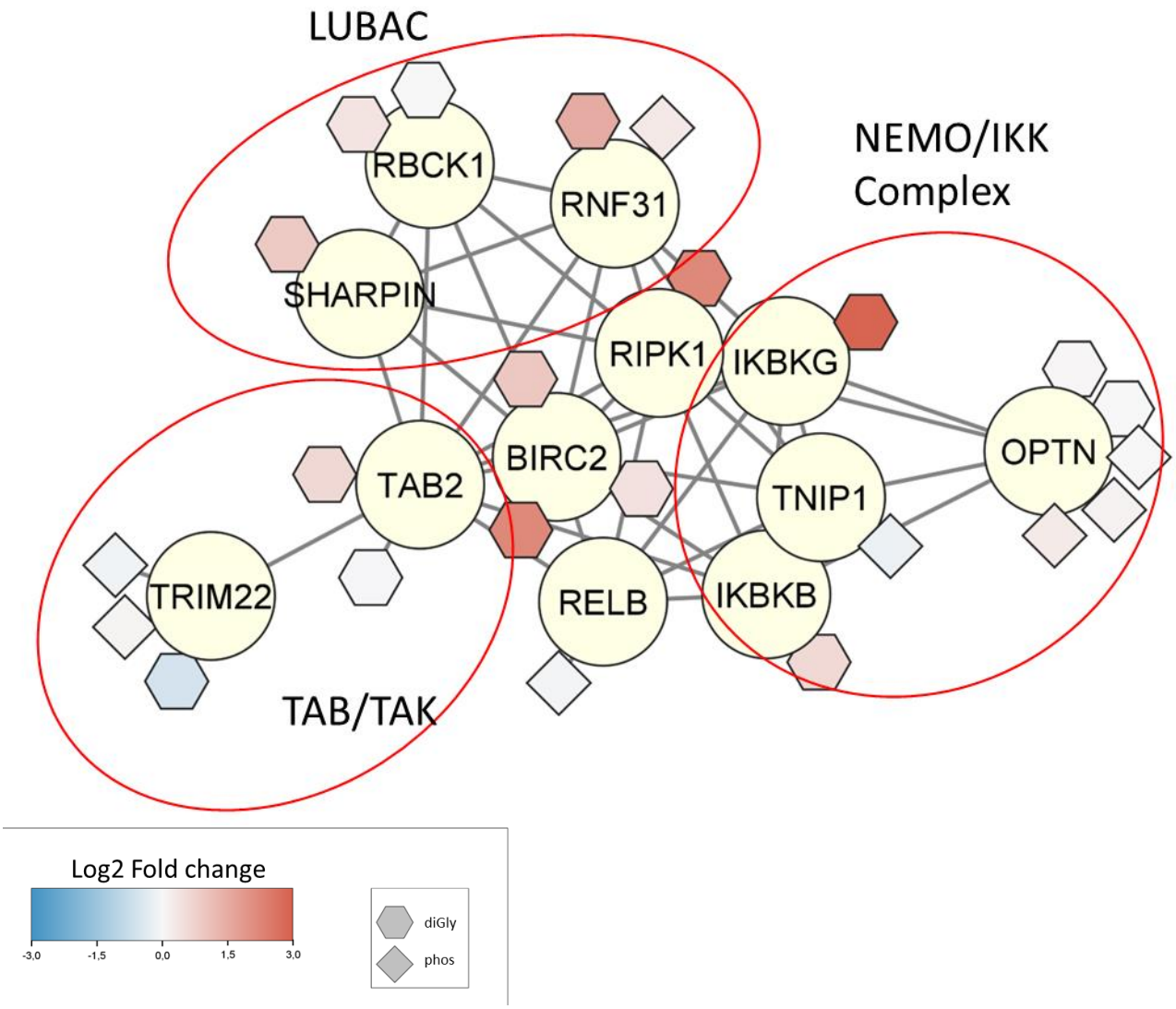

Supplementary Figure S4: Network of components of TNFR1 signaling as shown in Figure 1A. Hexagons represent ubiquitin sites and diamonds represent phosphorylation sites.